Oncogene (2013) **32,** 2058–2068
© 2013 Macmillan Publishers Limited All rights reserved 0950-9232/13
www.nature.com/onc

Open

ORIGINAL ARTICLE

Involvement of decreased hypoxia-inducible factor 1 activity and resultant G_1–S cell cycle transition in radioresistance of perinecrotic tumor cells

Y Zhu[1,2,3], T Zhao[1,2,4], S Itasaka[2], L Zeng[1,2,4], CJ Yeom[1], K Hirota[5], K Suzuki[6], A Morinibu[1], K Shinomiya[1], G Ou[2], M Yoshimura[2], M Hiraoka[2] and H Harada[1]

Cancer patients often suffer from local tumor recurrence after radiation therapy. Some intracellular and extracellular factors, such as activity of hypoxia-inducible factor 1 (HIF-1), cell cycle status and oxygen availability, have been suggested to affect DNA damage responses and eventual radioresistant characteristics of cancer cells. But when, where, and how these factors affect one another and induce cellular radioresistance is largely unknown. Here, we analyzed mechanistic and spatio-temporal relationships among them in highly heterogeneous tumor microenvironments. Experiments *in vitro* demonstrated that a decrease in the glucose concentration reduced the transcriptional activity of HIF-1 and expression of a downstream gene for the cell cycle regulator $p27^{Kip1}$ even under hypoxic conditions. Then, the proportion of cells in the radioresistant S phase increased, whereas that in the radiosensitive G_1 phase decreased, significantly. Immunohistochemical analyses showed that cancer cells in perinecrotic hypoxic regions, which should be under low-glucose conditions, expressed little HIF-1α, and therefore, were mainly in S phase and less damaged by radiation treatment. Continuous administration of glucagon, which increases the blood glucose concentration and so improves glucose availability in perinecrotic hypoxic regions, induced HIF-1α expression and increased radiation-induced DNA damage. Taken all together, these results indicate that cancer cells in perinecrotic regions, which would be under low-glucose and hypoxic conditions, obtain radioresistance by decreasing the level of both HIF-1 activity and $p27^{Kip1}$ expression, and adjusting their cell cycle to the radioresistant S phase.

Oncogene (2013) **32,** 2058–2068; doi:10.1038/onc.2012.223; published online 18 June 2012

Keywords: radiation therapy; radioresistance; tumor microenvironments; hypoxia; hypoxia-inducible factor 1 (HIF-1)

INTRODUCTION

Cancer patients often suffer from local tumor recurrence and distant tumor metastases after radiation therapy. It has been widely accepted that these problems are caused by the existence of radioresistant cancer cells in malignant solid tumors. Accumulated evidence has suggested that radioresistance is influenced by various intrinsic/intracellular and extrinsic/extracellular factors. One of the most influential extrinsic factors is hypoxia, an oxygen concentration below the physiological level.[1–4] Oxygen depletion is known to primarily disturb the production of reactive and cytotoxic species by ionizing radiation. Moreover, DNA radicals, which are barely produced under hypoxia through the ionization of DNA, can be chemically reduced by sulfhydryl group-containing materials, resulting in the prevention of DNA damage production. On the other hand, under oxygen-available conditions, molecular oxygen oxidizes the DNA radicals, leading to the formation of non-restorable DNA damage. These mechanisms are known as the chemical oxygen effect.[2,5] In addition, hypoxia is known to increase radioresistance of malignant solid tumors at a tissue level through some biological mechanisms as well. One of them is mediated by a transcription factor, hypoxia-inducible factor 1 (HIF-1). HIF-1 is reported to promote survival of endothelial cells after radiation therapy by inducing the expression of its downstream gene, vascular endothelial cell growth factor, and thus promote the overall radioresistance of tumors.[6–8] Actually, basic and clinical research have confirmed that increases of intratumoral hypoxia and HIF-1 activity correlate with a poor prognosis and incidences of both tumor recurrence and distant tumor metastasis after radiation therapy.[9–12]

HIF-1 is a heterodimeric transcription factor composed of an α-subunit (HIF-1α) and a β-subunit (HIF-1β). Its activity is mainly dependent on the stability of the former.[13] The oxygen-dependent degradation domain of HIF-1α is hydroxylated by prolyl hydroxylases in an oxygen-dependent manner. The modification triggers the ubiquitination of the subunit by pVHL-containing E3 ubiquitin ligase and subsequent proteolysis by the 26S proteasome complex.[14,15] Conversely, HIF-1α becomes relatively stable under hypoxic conditions, because the depletion of oxygen directly inactivates prolyl hydroxylases.[13] Then, HIF-1α interacts with HIF-1β to form an active heterodimer, HIF-1. HIF-1 binds to its cognate enhancer sequence, the hypoxia-responsive element (HRE), and induces the expression of various genes

[1]Group of Radiation and Tumor Biology, Career-Path Promotion Unit for Young Life Scientists, Kyoto University, Kyoto, Japan; [2]Department of Radiation Oncology and Image-applied Therapy, Kyoto University Graduate School of Medicine, Kyoto, Japan; [3]Department of Oncology, The First Affiliated Hospital of Chongqing Medical University, Chongqing, China; [4]Department of Radiation Medicine, Fourth Military Medical University, Shaanxi, China; [5]Department of Anesthesia, Kyoto University Hospital, Kyoto University, Kyoto, Japan and [6]Department of Radiology and Radiation Biology, Division of Radiation Biology, Graduate School of Biomedical Sciences, Nagasaki University, Nagasaki, Japan. Correspondence: Dr H Harada, Group of Radiation and Tumor Biology, Career-Path Promotion Unit for Young Life Scientists, Kyoto University, Yoshida Konoe-cho, Sakyo-ku, Kyoto, Japan.
E-mail: hharada@kuhp.kyoto-u.ac.jp
Received 6 December 2011; revised 3 April 2012; accepted 23 April 2012; published online 18 June 2012

related to the adaptation of cellular metabolism to hypoxia (the switch from oxidative to anoxic respiration),[16] escaping from hypoxia (invasion and metastasis of cancer cells),[17,18] improvements in hypoxia (angiogenesis)[19,20] and the resistance of malignant tumors to chemo as well as radiation therapy.

In terms of tumor biology, it is easy to understand how hypoxic regions can develop in malignant solid tumors. Cancer cells survive only in regions close to tumor blood vessels because of the limited distance that molecular oxygen and nutrients can diffuse. Consequently, most malignant tumors grow individually as a conglomerate of so-called tumor cords, in each of which a blood vessel is surrounded by, in order, well-oxygenated (normoxic), oxygen-insufficient (chronic/diffusion-limited hypoxic) and oxygen-depleted (necrotic) cancer cells.[3,21] Detailed immunohistochemical analyses with both an anti-HIF-1α antibody and a hypoxia marker, pimonidazole, recently revealed that chronic hypoxia is mainly composed of two layers; HIF-1α-positive/pimonidazole-negative (herein, HIF-1-positive) and pimonidazole-positive/HIF-1α-negative (pimonidazole-positive). The former occurs closer to tumor blood vessels where partial oxygen pressure is relatively high. The existence of these layers has been widely confirmed in various human tumors and tumor xenografts.[22–24] The mechanism behind the generation of the two layers remains to be elucidated; however, it is likely to depend on the difference in Km values for the stabilization of the HIF-1α protein and for the formation of the pimonidazole adduct. In addition, decreased glucose availability in the pimonidazole-positive layer because of the limited distance glucose can diffuse from blood vessels is also suggested to reduce HIF-1α levels there.

It is known that cell cycle progression is inhibited at the G_1 phase under hypoxic conditions in many, but not all, types of cells.[25] However, because this phase is considered relatively radiosensitive (Supplementary Figure S1),[26] hypoxia-mediated G_1 arrest sounds somewhat inconsistent with the notion of increased radioresistance under hypoxic conditions.[9–11] Therefore, it becomes increasingly important to analyze the spatio-temporal relationship among cell cycle status, cellular radioresistance and hypoxic regions in highly heterogeneous tumor microenvironments. Also, the function of HIF-1 in these relationships is interesting.

Here, we demonstrate that, in addition to the radiation chemical mechanism mediated by oxygen depletion, a biological mechanism mediated by the decrease in HIF-1 activity, at least in part, contributes to the radioresistance of pimonidazole-positive tumor cells. Namely, we found that the reduced expression of HIF-1α, which is caused by low-glucose availability under hypoxic conditions, leads to a decrease in the expression of a cell cycle regulator, $p27^{Kip1}$, and transition from the radiosensitive G_1 to radioresistant S phase.

RESULTS

Relationship between cell cycle status and tumor microenvironments

It has been found through experiments *in vitro* that oxygen availability and cell cycle status each influences the radiosensitivity of cancer cells.[2,26,27] An ~1.3–2.0 times higher dose of radiation is needed to kill late S-phase cells to the same extent as G_1-phase cells (Supplementary Figure S1).[26,27] Meanwhile, the ratio of radiation dose necessary to produce the same level of cell killing effect under hypoxic conditions to that under normoxic conditions is ~3.0–3.5 (dependent on the dose of radiation).[2,28] However, how and where these two factors influence each other in highly heterogeneous malignant tumors and produce radioresistant cancer cells remain largely unknown. Here, we first performed immunohistochemical analyses with intrinsic and extrinsic markers of hypoxia, HIF-1α and pimonidazole, respectively, and with an S-phase marker, Cyclin A (Figure 1; Supplementary Figure S2, S3). Hypoxic regions were detected with both markers in areas far from perfusion-positive tumor blood vessels (Figure 1a; Supplementary Figure S3A). HIF-1α-positive areas were slightly but definitely closer to blood vessels than pimonidazole-positive areas, consistent with previous reports.[23,24] Cancer cells with high levels of Cyclin A were detected predominantly in pimonidazole-positive regions in addition to in normoxic regions, but not in HIF-1α-positive regions (Figures 1b and c; Supplementary Figure S3B and C). Immunostaining with a proliferation marker, BrdU, confirmed that, although normoxic tumor cells are proliferative, pimonidazole-positive cells are not (Supplementary Figure S4). These results indicate that hypoxic but not HIF-1α-positive conditions increase the number of non-proliferative S-phase cells in pimonidazole-positive perinecrotic regions.

G_1–S transition under hypoxic and low-glucose conditions

To explore the mechanism behind the increase in S-phase cells in pimonidazole-positive/HIF-1-negative hypoxic regions (herein, pimonidazole-positive regions), we examined the influence that the extent of oxygen depletion has on cell cycle status. As HIF-1 is reported to function in cell cycle regulation under hypoxic conditions[25] and because $p27^{Kip1}$ is an important factor arresting the cell cycle at the G_1 checkpoint,[29] we examined their involvement as well. To monitor the transcriptional activity of HIF-1, we used HeLa/5HRE-Luc cells, which express the luciferase protein under the control of a HIF-1-dependent 5HRE promoter.[30] The HIF-1α expression, HIF-1 activity, and $p27^{Kip1}$ expression increased as the oxygen concentration decreased (Figure 2a). The increase in $p27^{Kip1}$ accompanied G_1 arrest under hypoxic conditions, but no transition from G_1 to S (Figures 2b and c; Supplementary Figure S5).

We next examined the influence of a decreased glucose concentration on cell cycle status under hypoxia *in vitro,* because cancer cells would be exposed to low-glucose as well as hypoxic conditions in regions far from tumor blood vessels such as the pimonidazole-positive layer.[31,32] A decrease in the glucose concentration led to the suppression of HIF-1α expression, HIF-1 activity and $p27^{Kip1}$ expression even under hypoxic conditions (Figures 3a–c: lanes 5 and 6), and then, resulted in a decrease and increase in the proportion of G_1- and S-phase cells, respectively (Figures 3d–g). Knockdown of HIF-1α expression resulted in a significant reduction in the level of $p27^{Kip1}$ as well as one of the most representative downstream genes of HIF-1, carbonic anhydrase IX (*CA9*), indicating the dependency of $p27^{Kip1}$ expression on HIF-1 (Supplementary Figure S6).

To directly examine the importance of the decreased HIF-1 activity in the G_1–S transition, we utilized pcDNA3/HIF-1α-CA. The plasmid expresses a constitutively active HIF-1α (HIF-1α-CA), a mutant lacking the oxygen-dependent degradation domain because of the deletion of residues 330–575. The forced expression of HIF-1α-CA almost completely abrogated the suppression of HIF-1 activity and $p27^{Kip1}$ expression caused by the decrease in the glucose concentration under hypoxic conditions (Figures 3a–c: lane 8). The abrogation resulted in a recovery of the proportion of G_1-phase cells (Figures 3d–g).

To examine the involvement of decreased $p27^{Kip1}$ levels in the G_1–S transition under low-glucose and hypoxic conditions, we next employed a plasmid expressing a fusion protein, $p27^{Kip1}$-myc epitope tag, under the transcriptional control of the CMV promoter. Overexpression of $p27^{Kip1}$ also canceled the G_1–S transition and increased the proportion of G_1-phase cells under low-glucose and hypoxic conditions (Figure 4a–e, lane 8).

We next tested whether insufficient glucose availability is actually responsible for the decreased expression of HIF-1α in pimonidazole-stained cells of tumor xenografts. In order to increase the concentration of glucose in the pimonidazole-

© 2013 Macmillan Publishers Limited

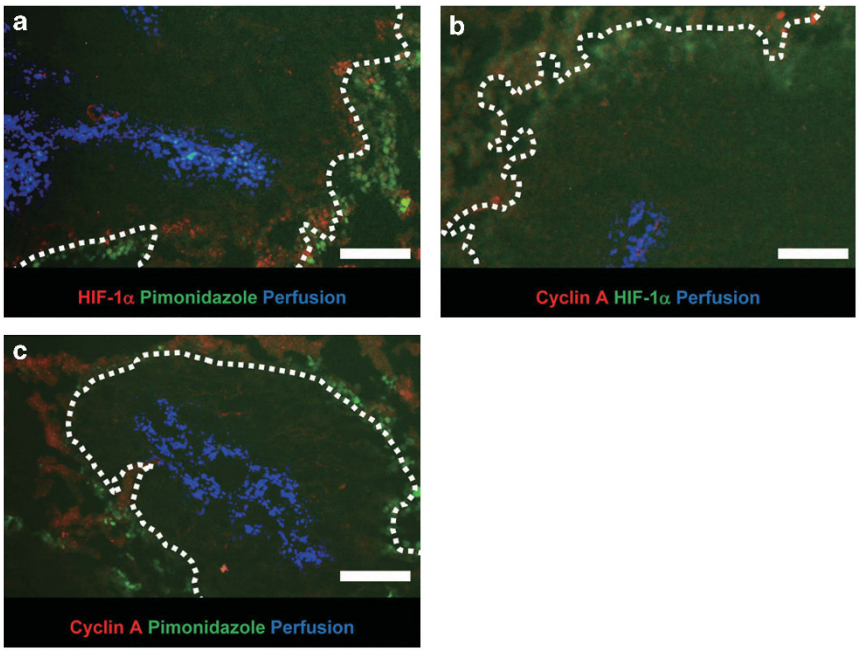

Figure 1. Cell cycle status in pimonidazole-positive/HIF-1-negative and HIF-1-positive/pimonidazole-negative hypoxic regions of tumor xenografts. Frozen sections of HeLa tumor xenografts were stained with the indicated combination of antibodies against a hypoxia marker, pimonidazole (green in **a**, **c**), HIF-1α (red in **a** and green in **b**) and cyclin A (red in **b** and **c**). Representative pictures are shown. Blue = perfusion marker, hoechst 33342. Bar = 50 μm. Dotted lines are inside edges of the pimonidazole-positive/HIF-1-negative regions (**a**, **c**) and outside edges of the HIF-1-positive/pimonidazole-negative regions (**b**) in each tumor cord.

positive regions, we applied an osmotic pump to tumor-bearing mice and continuously administered glucagon, a hormone raising blood glucose levels (Figure 5).[33,34] And then we analyzed the HIF-1α level in pimonidazole-positive cells. Consistent with the above data (Figure 1a), HIF-1α-positive regions were located closer to tumor blood vessels than pimonidazole-positive regions in the xenograft tumors without glucagon treatment (Figure 5, upper). On the other hand, glucagon treatment dramatically induced the expression of HIF-1α in pimonidazole-positive cells (Figure 5, lower). The *in vivo* data indicate that glucose could diffuse only to closer hypoxic regions and is responsible for the HIF-1α expression there. On the other hand, the *in vivo* data combined with results of a series of *in vitro* experiments indicate that a decreased glucose concentration in regions relatively distant from tumor blood vessels leads to G_1–S transition through the suppression of HIF-1α expression, HIF-1 activity and $p27^{Kip1}$ expression.

Decrease in radiation-induced DNA damage under hypoxic and low-glucose conditions

Cell cycle status is known to influence the radiosensitivity/radioresistance of cells. Namely, cells are radioresistant in S phase.[27] To test whether the G_1–S transition under low-glucose and hypoxic conditions leads to cellular radioresistance, we employed p53-binding protein 1 (53BP1)[35–37] and γH2AX, a member of the histone H2A family phosphorylated at serine 139,[38–40] as markers of DNA damage.

The 53BP1 protein is known to re-localize to form foci that are recognized as sites of DNA lesions.[35–37] The minimum domain of 53BP1 essential for accumulating at damaged sites was identified as residues 1220–1703 and called the 53BP1-M domain.[41] We constructed a plasmid expressing the fusion protein EGFP–53BP1-M under the control of a constitutively active CMV promoter. We established a stable cell line with the plasmid and irradiated the cells to examine the influence of glucose and/or oxygen availability on the DNA damage (Figure 6). The number of 53BP1-M foci significantly decreased under hypoxic conditions compared with normoxic conditions, consistent with the oxygen effect (Figure 6a). The number of radiation-induced foci further diminished as a result of a decreasing glucose concentration under hypoxic conditions.

We next employed γH2AX as a marker of DNA lesions[38–40] and performed a quantitative experiment using two cell lines (A549 and HEK293) after radiation treatment *in vitro* (Figures 6b and c). Radiation induced the same amount of phosphorylation of H2AX (γH2AX) regardless of the glucose concentration under normoxic conditions (Figures 6b and c: lanes 2 and 4). The signal intensity of γH2AX markedlly decreased under hypoxic as compared with normoxic conditions (Figures 6b and c: lane 6). The decrease in the glucose concentration further reduced the γH2AX level under hypoxic conditions (Figures 6b and c: lane 8).

To directly examine the involvement of the decreased $p27^{Kip1}$ expression in the reduction of radiation-induced DNA damage under low-glucose and hypoxic conditions, we performed the 53BP1 focus assay again with or without the overexpression of $p27^{Kip1}$ (Figure 6d). The transient overexpression of $p27^{Kip1}$ almost completely restored the number of 53BP1 foci to that under high-glucose and hypoxic conditions (See Figure 6d: lanes 6 and 8), meaning that the reduction in DNA damage caused by the reduced glucose concentration was fully mediated through the decrease of $p27^{Kip1}$.

To examine whether the G_1–S transition and resultant decrease in DNA damage actually lead to radioresistance of cancer cells, we next performed a clonogenic survival assay *in vitro*. HeLa cells were exposed to 0, 2, 4 or 8 Gy of X-ray irradiation in the presence of high or low concentrations of glucose under normoxic or hypoxic conditions (Figure 6e). The reduction of glucose availability significantly increased cellular radioresistance under hypoxic conditions. The dose of radiation needed to kill 50% of cells under the low-glucose and hypoxic conditions was 1.70 times higher than that under the high-glucose and hypoxic conditions (6.3 Gy vs 3.7 Gy for the low and high concentration of glucose, respectively). All of these results indicate that cancer cells obtain radioresistant characteristics under low-glucose and hypoxic

© 2013 Macmillan Publishers Limited

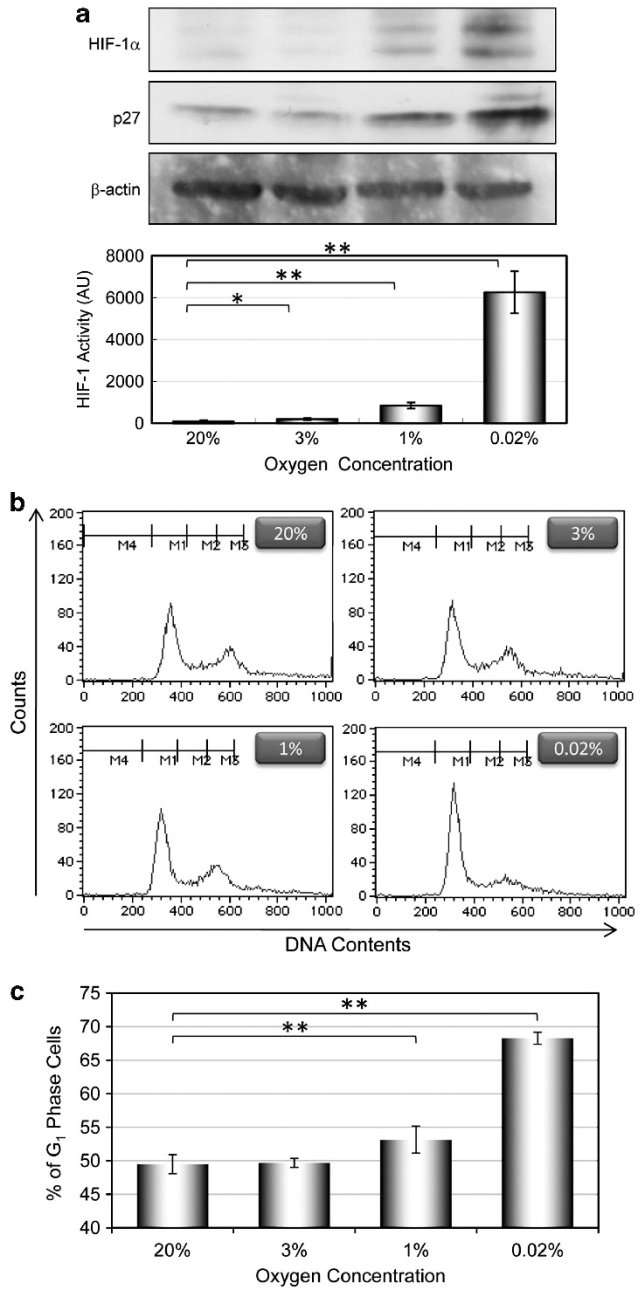

Figure 2. Increase in the proportion of G_1 cells under hypoxic conditions. (**a**–**c**) HeLa/5HRE-Luc cells were cultured under normoxic (20%) or hypoxic (3, 1 and 0.02%) conditions for 20 h. (**a**) Cell lysate was subjected to western blotting for HIF-1α, $p27^{Kip1}$ and β-actin (upper) and a luciferase assay (lower). Results are the mean ± s.d. $n = 3$. $^*P < 0.05$. $^{**}P < 0.01$. (**b**, **c**) The cell suspensions were subjected to flow cytometry for cell cycle analyses. (**b**) Representative data for each treatment group are shown. (**c**) Proportions of cells in the G_1 phase were quantified based on the data in Figure 2b. Results are the mean ± s.d. $n = 3$. $^{**}P < 0.01$.

conditions through G_1–S transition mediated by a decrease in $p27^{Kip1}$ expression.

Decrease in radiation-induced DNA damage in pimonidazole-positive regions of solid tumors

We examined whether cells in pimonidazole-positive hypoxic regions are actually resistant to radiation *in vivo*. HeLa tumor xenografts were treated with 4 Gy of X-radiation, and 30 min later surgically excised for immunohistochemical analysis with a combination of antibodies against pimonidazole and γH2AX (Figure 7; Supplementary Figure S7). The number of γH2AX foci was obviously decreased in pimonidazole-positive regions compared with regions close to tumor blood vessels (Figure 7). To directly examine the involvement of the low-glucose-mediated biological mechanism in the radioresistance of pimonidazole-positive cells, we treated tumor-bearing mice with glucagon and increased the levels of glucose and HIF-1α in pimonidazole-positive regions (Figure 5). Then, we analyzed the extent of DNA damage caused by radiation treatment in pimonidazole-positive regions and pimonidazole-negative regions (regions excluding pimonidazole-positive regions and necrotic regions) (Figure 8). Compared with the radiation-induced increase of γH2AX-positive cells in pimonidazole-negative regions (27.3% = 45.2%–17.9%), that in pimonidazole-positive regions (12.1% = 23.4%–11.3%) was significantly less (Figure 8). The percent reduction of DNA damage in pimonidazole-positive regions was 55.7% ((27.3 − 12.1)/27.3 × 100%). On the other hand, after the glucagon treatment, the radiation-induced increase of γH2AX-positive cells in pimonidazole-negative and pimonidazole-positive regions was 33.3% (53.0%–19.7%) and 18.0% (34.1%–16.1%), respectively. The percent reduction of DNA damage in pimonidazole-positive regions was 45.9% ((33.3–18.0)/33.3 × 100%). On the basis of these analyses, at least 17.6% ((55.7–45.9)/55.7 × 100%) of the radioresistance of pimonidazole-positive cells would be dependent on the low-glucose-mediated biological mechanism. These results suggest that the low-glucose-mediated biological mechanism, in addition to the oxygen-mediated radiation chemical mechanism, certainly has an important role in the radioresistance of pimonidazole-positive cells.

DISCUSSION

In the present study, we analyzed how some extrinsic and intrinsic factors influence one another and cause radioresistant cancer cells in highly heterogeneous tumor microenvironments. We especially focused on the influence of the spatial relationship among oxygen-/glucose availability, HIF-1α expression, HIF-1 activity and cell cycle distribution on radioresistant characteristics of cancer cells. We then successfully unveiled a mechanism whereby transition from the radiosensitive G_1 to radioresistant S phase of the cell cycle is mediated by the decreased expression of HIF-1α and $p27^{Kip1}$ in perinecrotic/pimonidazole-positive regions of malignant solid tumors and has an important role in the biological radioresistance of cancer cells there.

It is widely accepted that radiation biological as well as radiation chemical mechanisms have critical roles in the radioresistance of malignant tumors. Among various intrinsic and extrinsic factors, hypoxia and HIF-1 have received considerable attention in recent years, because they have been reported to correlate with a poor prognosis and the incidence of both local tumor recurrence and distant tumor metastasis after radiation therapy.[9–11] Against this background, hypoxia has been reported to induce cell cycle arrest at the relatively radiosensitive G_1 phase (Supplementary Figure S1).[25–27] This discrepancy can be resolved here by considering the involvement of decreased HIF-1 activity in perinecrotic regions. Our data suggest that most cancer cells in pimonidazole-positive regions are HIF-1α-negative in HeLa tumor xenografts. The downregulation of HIF-1 activity leads to a transition from G_1 to S as a result of the suppression of $p27^{Kip1}$ expression. The G_1–S transition induces resistance to radiation-induced DNA damage, resulting in enhanced survival after treatment. This model seems reasonable, but several issues remain to be addressed. First, it is not completely clear how HIF-1α expression is suppressed under low-glucose and hypoxic conditions. Second, it is also unknown how the cell cycle was arrested at the S phase after the G_1–S transition under low- glucose and hypoxic conditions.

© 2013 Macmillan Publishers Limited

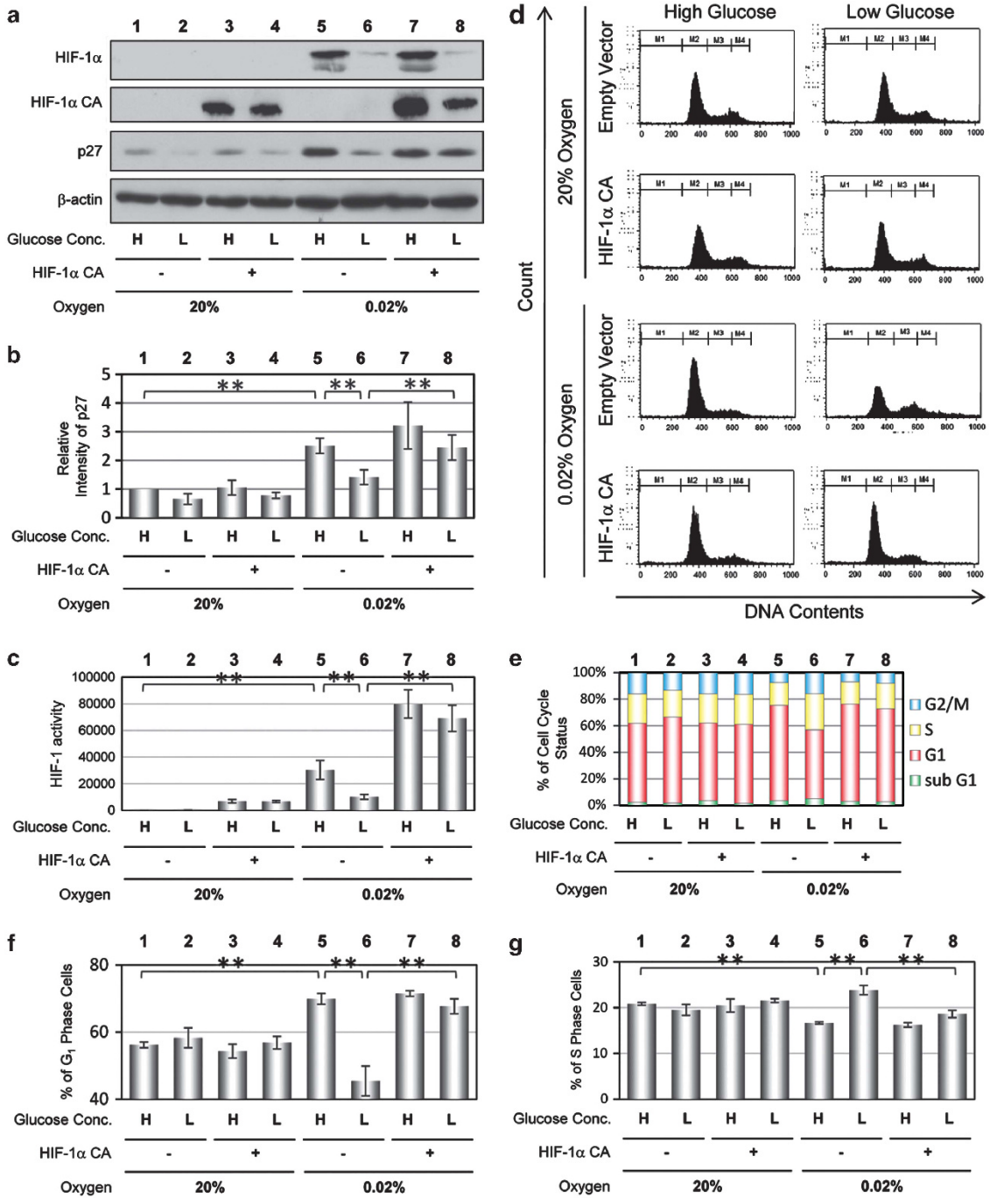

Figure 3. Involvement of decreased HIF-1 activity in the transition from the G_1 to S phase under low-glucose and hypoxic conditions. HeLa/5HRE-Luc cells were transiently transfected with pcDNA3.1/myc-HIS (empty vector: EV) or pcDNA3/HIF-1α-CA and cultured for 24 h. They were then cultured in fresh medium containing a low (L: 0.45 g/l) or high (H: 4.5 g/l) concentration of glucose under normoxic (20% oxygen) or hypoxic (0.02% oxygen) conditions for 20 h. (**a)** Cell lysate was subjected to western blotting for HIF-1α, HIF-1α-CA, $p27^{Kip1}$ and β-actin. (**b)** The intensity of the bands was quantified using ImageJ. Results are the mean ± s.d. $n = 3$. $^{**}P < 0.01$. (**c**), Cell lysate was subjected to a luciferase assay. Results are the mean ± s.d. $n = 3$. $^{**}P < 0.01$. (**d–g)** Cell suspensions were subjected to flow cytometry for cell cycle analyses. (**d)** Representative data for each treatment group are shown. (**e–g)** Proportions of cells in the sub G_1, G_1, S and G_2/M phases (**e**) G_1 phase only (**f**) and S-phase only (**g**) were quantified based on the data in Figure 3d. Results are the mean ± s.d. $n = 3$. $^{**}P < 0.01$.

Third, although S-phase cells are known as relatively radioresistant, the molecular mechanism behind their resistance remains largely unknown. Finally, some aspects of this model remain to be proven. Assessing these issues has the potential to lead to the development of novel treatment strategies to overcome tumor radioresistance.

Here, we revealed the importance of sequential decreases of HIF-1α and $p27^{Kip1}$ levels in the G_1–S cell cycle transition and resultant radioresistance of pimonidazole-positive cells by thoroughly performing experiments. Dependence of $p27^{Kip1}$ expression on HIF-1 was directly confirmed by both knockdown of HIF-1α (Supplementary Figure S6) and overexpression of

© 2013 Macmillan Publishers Limited

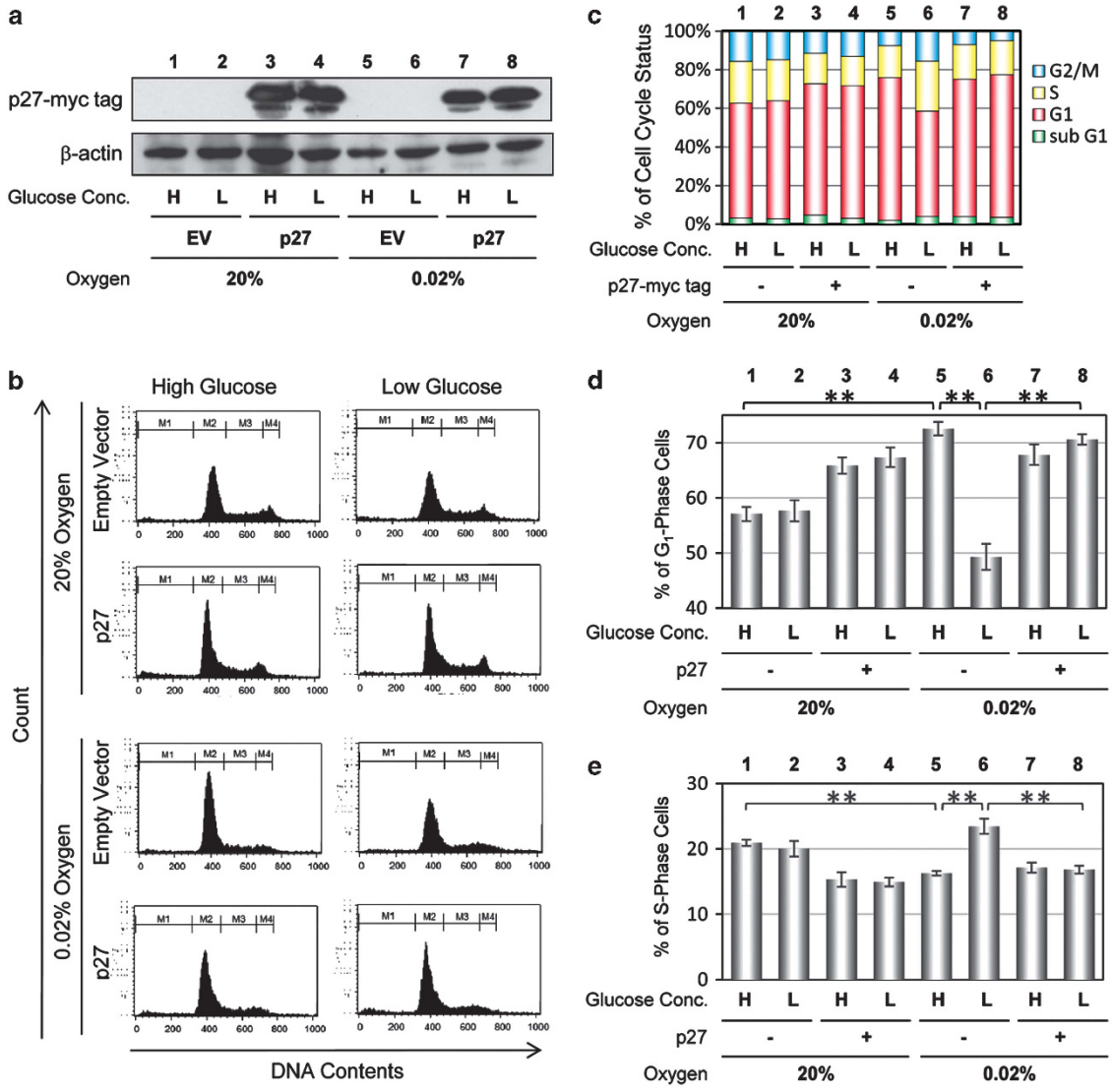

Figure 4. Involvement of decreased p27^{Kip1} expression in the transition from the G_1 to S phase under low-glucose and hypoxic conditions. HeLa/5HRE-Luc cells were transiently transfected with pcDNA4/myc-HIS (empty vector: EV) or pcDNA4/p27^{Kip1} and cultured for 24 h. They were then cultured in fresh medium containing a low (L: 0.45 g/l) or high (H: 4.5 g/l) concentration of glucose under normoxic (20% oxygen) or hypoxic (0.02% oxygen) conditions for 20 h. **(a)** Cell lysate was subjected to western blotting for p27^{Kip1} and β-actin. (**b**–**e)** Cell suspensions were then subjected to flow cytometry for cell cycle analyses. **(b)** Representative data for each treatment group are shown. (**c**–**e)** Proportions of cells in the sub G_1, G_1, S and G_2/M phases (**c**), G_1 phase only (**d**) and S-phase only (**e**) were quantified based on the data in **b**. Results are the mean ± s.d. $n = 3$. $^{**}P < 0.01$.

HIF-1α-CA (Figure 3). Likewise, involvement of decreased p27^{Kip1} levels in the G_1–S cell cycle transition under low-glucose and hypoxic conditions was also directly confirmed by the result that the proportion of G_1-phase cells was recovered by the forced expression of p27^{Kip1} (Figure 4). However, this mechanism seems somewhat inconsistent with previous reports that p27^{Kip1} expression was induced under hypoxia in a HIF-1-independent manner[42] and hypoxia-induced G_1 arrest is independent of p27^{Kip1}.[43] Further studies are needed to fully elucidate the molecular mechanism behind the cell-cycle regulation of pimonidazole-positive cells.

Pimonidazole-positive regions should be under severe hypoxia than HIF-1-positive regions because of the distance from tumor blood vessels.[21,23] So, pimonidazole-positive cancer cells should be more radioresistant than HIF-1-positive cells because of the so-called oxygen effect through the radiation chemical mechanism. In addition, the present study demonstrates that the decrease in HIF-1 activity actively induces the biological radioresistance of cancer cells through G_1–S transition in pimonidazole-positive regions. If this is so, why has the expression of HIF-1α been reported to correlate with a poor prognosis and the incidence of both local tumor recurrence and distant tumor metastasis after radiation therapy?[9–11] The answer may lie in the relationship between the volume of pimonidazole-positive cells and that of HIF-1α-positive cells in malignant solid tumors. Namely, because pimonidazole-positive regions are generally accompanied by HIF-1α-positive regions, the volume of HIF-1α-positive regions may simply reflect that of pimonidazole-positive regions and eventually a poor prognosis and so on.

An important question raised from the present study is the relative contribution of the radiation chemical mechanism and the low-glucose-mediated biological mechanism in the radioresistance of pimonidazole-positive cells in malignant tumors. Our experiments *in vivo* using glucagon revealed at least 17.6% of the radioresistance of pimonidazole-positive cells to be dependent on the low-glucose-mediated biological mechanism. The same tendency was confirmed

© 2013 Macmillan Publishers Limited

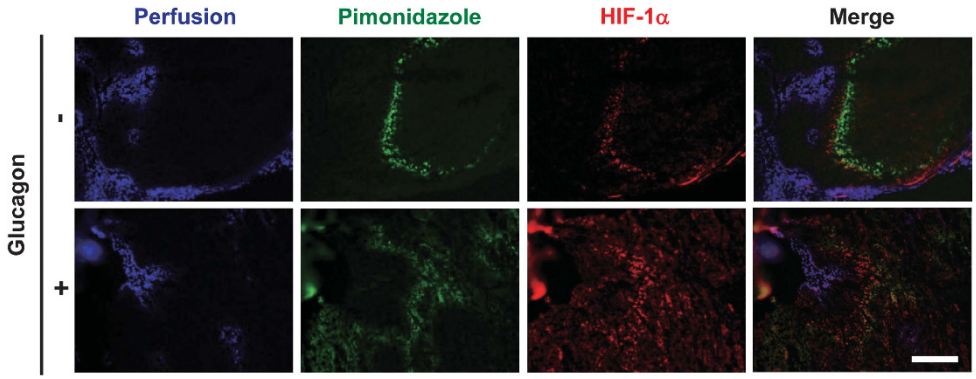

Figure 5. Increase of HIF-1α expression in pimonidazole-positive regions after glucagon-mediated improvement of glucose availability. HeLa tumor-bearing mice were continuously administered with (+) or without (−) glucagon for 5 days via an osmotic pump (See Materials and methods section for details). Then, the tumor xenografts were surgically excised, frozen in OCT compound and subjected to immunohistochemical analysis with a hypoxia marker, pimonidazole (green) and anti-HIF-1α antibody (red). The tumor-bearing mice were injected with the hypoxia marker and a perfusion marker, hoechst 33342, at 90 and 1 min before killing, respectively. Blue = perfusion marker, hoechst 33342. Bar = 100 μm.

in an *in vitro* experiment as well (Figure 6). Based on the results, we confirmed the importance of the biological mechanism although its contribution to the radioresistance seems relatively low.

Although the present study focused on the importance of decreased HIF-1α-expression to the radioresistance of pimonidazole-positive cells, one should not ignore the importance of HIF-1 as a therapeutic target in radiation therapy. It has been reported that HIF-1 becomes active in response to radiation treatment in malignant solid tumors, functions to protect tumor blood vessels from cytotoxic effects of radiation by inducing the expression of vascular endothelial cell growth factor, assures the delivery of oxygen and nutrients to cancer cells, and eventually accelerates tumor growth after the treatment.[6,7,44] So, a blockade of the radiation-induced activation of HIF-1 enhances the therapeutic effect of radiation. Taken together, the parameters most important for effective radiation therapy are the volume of pimonidazole-positive hypoxia (absolute hypoxia) before radiation and the volume of HIF-1α-positive regions and intratumoral HIF-1 activity after radiation.

The present study provides a clue as to how to optimize regimens for combined treatment with radiation therapy and a HIF-1 inhibitor. Our findings suggest that when administered before radiation, a HIF-1 inhibitor would increase the radioresistance of HIF-1α-positive cancer cells by inducing a transition from the radiosensitive G_1 to radioresistant S phase. This notion is consistent with our previous report that inhibition of HIF-1 activity before radiation therapy suppressed rather than enhanced the therapeutic effect.[45] Therefore, one can achieve the best therapeutic effect by administering a HIF-1 inhibitor to suppress the radiation-induced activation of HIF-1 only.

An important question arising from the present study is how to overcome the radioresistance of pimonidazole-positive cells which show low HIF-1 activity under low-glucose and hypoxic conditions. The administration of glucagon may be able to cancel the radioresistance by restoring HIF-1α expression and HIF-1 activity and arresting the cell cycle at the radiosensitive G_1 phase. The treatment, however, may simultaneously stimulate the growth of cancer cells in both normoxic and HIF-1α-positive hypoxic regions. An alternative seems to be a combination of radiation therapy and a hypoxia cytotoxin such as tirapazamine,[46] whose cytotoxicity is fully dependent on absolute low oxygen tension. Moreover, based on the present study, the therapeutic effect of the triple combination of radiation therapy, a hypoxia cytotoxin (for the effective killing of pimonidazole-positive cells) and a HIF-1 inhibitor (for the suppression of radiation-induced activation of HIF-1) should be also examined.

MATERIALS AND METHODS

Cell culture and reagents

The human cervical epithelial adenocarcinoma cell line (HeLa), human lung carcinoma cell line (A549) and Human Embryonic Kidney 293 cell line (HEK293) were purchased from American Type Culture Collection (Manassas, VA, USA). Cells were cultured in 10% FBS-containing Dulbecco's modified Eagle's medium (DMEM) with a high (4.5 g/l) or low (0.45 g/l) concentration of glucose. HEK293 cells were cultured in type I collagen-coated culture dishes (AGC Techno Glass Co. Ltd., Chiba, Japan). Cells were incubated in a well-humidified incubator with 5% CO_2 and 95% air at 37 °C for normoxic cultures. Alternatively, cells were incubated in a Bactron Anaerobic Chamber, BACLITE-2 (Sheldon Manufacturing Inc., Cornelius, OR, USA), for the $<0.02\%$ O_2 condition, in a multi-gas incubator (MCO-5M, Sanyo, Tokyo, Japan) for the 3% O_2 condition, or in an Invivo$_2$ 500 Hypoxia workstation (Ruskinn Technology Limited, Bridgend, UK) for the 1% O_2 condition. The concentration of hydroxyurea for synchronization of the cell cycle *in vitro* was 1 mM in PBS. Glucagon was dissolved with 3.44 M of cetrimid solution at a working concentration of 2 mg/ml for the *in vivo* study.

Plasmid DNA

The plasmid pEF/5HRE-Luc harboring a *5HREp-luc* reporter gene, which expresses luciferase under the control of a HIF-1-dependent 5HRE promoter, was constructed as described previously.[30] To construct the plasmid pEGFP-53BP1-M, the coding sequence of the M domain of the p53-binding protein 1 (*53BP1*) gene, which comprises residues 1220–1703 and is responsible for the recruitment of 53BP1 to DNA double-stranded breaks,[41] was amplified by PCR and inserted between the *Xho*I-*Hind*III sites of pEGFP-C1 (Clontech, Palo Alto, CA, USA). To construct the plasmid pcDNA4/p27^{Kip1}, the coding sequence of the *p27^{Kip1}* gene was amplified by PCR and inserted between the *Eco*RI-*Xho*I sites of pcDNA4/myc-His A (Invitrogen Corp., Carlsbad, CA, USA). The plasmid pcDNA3-HIF-1α-CA, which expresses a constitutively active mutant form of HIF-1α (HIF-1α-CA) lacking the oxygen-dependent degradation domain because of the deletion of residues 330–575, was kindly provided by Dr GL Semenza.

Isolation of stable transfectants

The HeLa/5HRE-Luc cell line was established as described previously.[30] For the establishment of the 293/EGFP-53BP1-M cell line, HEK293 cells were stably transfected with pEGFP-53BP1-M by the calcium phosphate method,[47] and cultured for 14 days in medium containing 400 μg/ml of G418 (Nacalai Tesque, Kyoto, Japan). Antibiotic-resistant colonies showing radiation-dependent EGFP-53BP1-M were isolated and established as clones. A representative clone was used in this study.

Transient transfection

Cells were transiently transfected with pcDNA3.1/myc-His (as an empty vector (EV); Invitrogen Corp.) or pcDNA3-HIF-1α-CA (in Figure 3), or with

© 2013 Macmillan Publishers Limited

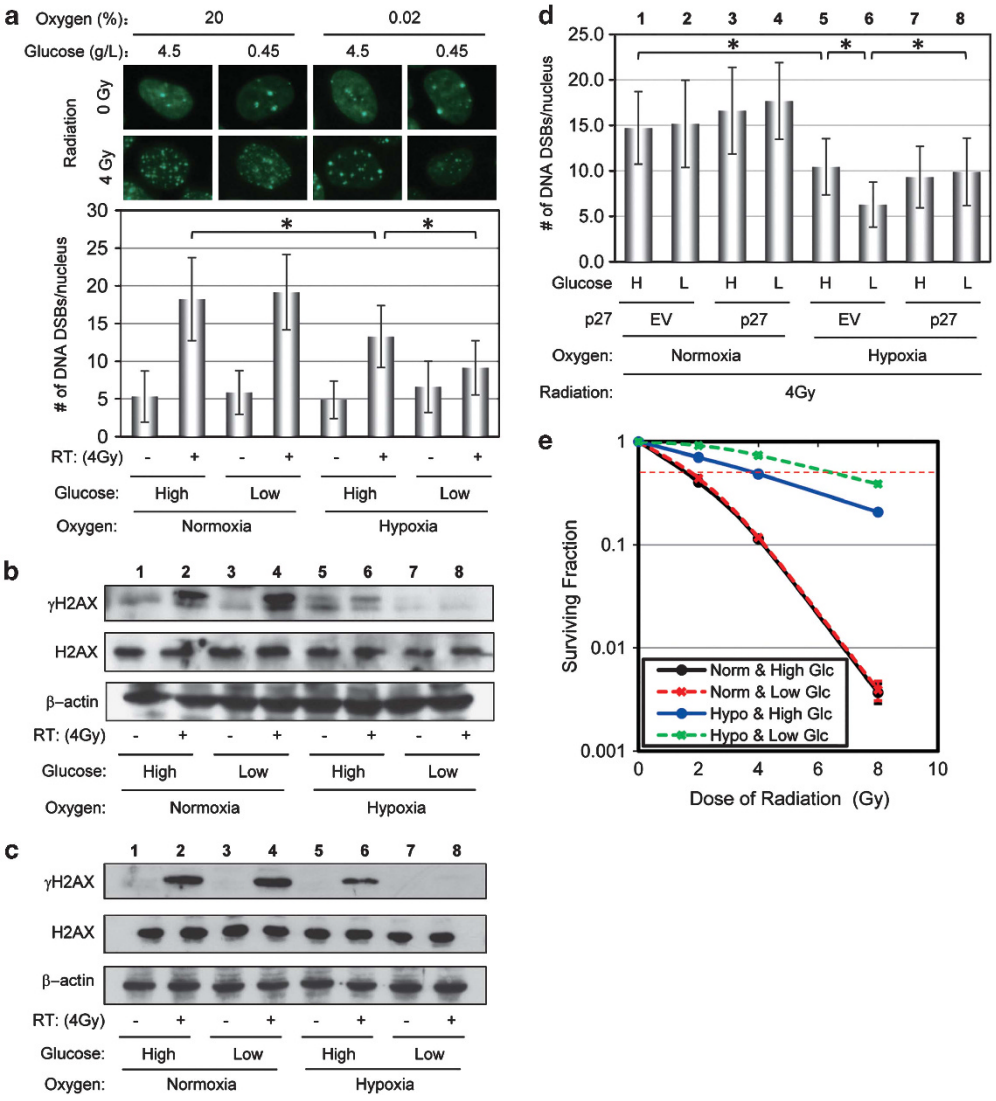

Figure 6. Radioresistance of cells under low-glucose and hypoxic conditions. (**a**–**e**) With (**d**) or without (**a**–**c**, **e**) transient transfection using an empty vector or pcDNA4/p27^{Kip1}, HEK293/EGFP-53BP1-M (**a**, **b**, **d**, **e**) and A549 (**c**) cells were cultured in medium containing a low (L: 0.45 g/l) or high (H: 4.5 g/l) concentration of glucose under normoxic (20% oxygen) or hypoxic (0.02% oxygen) conditions for 20 h, and treated with the indicated dose of X-radiation. (**a**, **d**) The radiation-induced DNA double-stranded breaks (DNA DSBs) were then observed as EGFP-53BP1-M foci under a fluorescence microscope. The numbers of DNA DSB per nucleus in each group were quantified as the mean of 50 nuclei in 10 independent fields. Results are the mean ± s.d. *$P<0.05$. (**b**, **c**) Cell lysate was subjected to western blotting for γH2AX, H2AX and β-actin. (**e**) The cells were subjected to a clonogenic cell survival assay. *X* axis = dose of X-radiation. *Y* axis = surviving fraction. $n=3$. Results are the mean ± s.d. *Note*: error bars are invisible in some groups because they are smaller than the size of icons.

pcDNA4/myc-His (as an empty vector (EV); Invitrogen Corp.) or pcDNA4/p27^{KIP1} (in Figures 4 and 6d) using the Polyfection transfection reagent (Qiagen Inc., Valencia, CA, USA) according to the manufacturer's instructions. The cells were then cultured for 24 h and subjected to each *in vitro* experiment.

Luciferase assay, western blotting and flow cytometric analyses

HeLa/5HRE-Luc cells were seeded in 24-well plates for luciferase assays (1×10^5 cells/well) or in 6-well plates for both western blotting and flow cytometric analyses (2×10^5/well). The cells were cultured in medium containing a high (4.5 g/l) or low (0.45 g/l) concentration of glucose for 20 h under various oxygen conditions as described in the figure legends. Cell lysate prepared with 100 μl of Passive Lysis Buffer (Promega, Madison, WI, USA) was subjected to an assay using Luciferase Assay Reagent (Promega) according to the manufacturer's instructions. Cell lysate prepared with CelLytic M cell lysis reagent (Sigma-Aldrich, St Louis, MO, USA) was subjected to western blotting for the detection of endogenous HIF-1α and exogenous HIF-1α-CA with an anti-human HIF-1α mouse monoclonal antibody (BD Bioscience, San Diego, CA, USA), endogenous β-actin with an anti-human β-actin mouse monoclonal antibody (BioVision Research Products, Mountain View, CA, USA), endogenous p27^{Kip1} with an anti-human p27^{Kip1} rabbit monoclonal antibody (Abcam, Cambridge, UK), exogenous p27^{Kip1}-myc-tag with an anti-myc-tag mouse monoclonal antibody (Cell Signaling Technology Inc., Beverly, MA, USA), endogenous H2 AX with an anti-human H2AX rabbit polyclonal antibody (Cell Signaling Technology Inc.) and endogenous γH2AX with an anti-human γH2AX rabbit antibody (#2577, Cell Signaling Technology Inc.) as described previously.[30,45,48,49] Before SDS–PAGE and western blotting, the protein concentration of each cell lysate was adjusted to 20 mg protein/20 μl by performing a protein assay using Quick Start Bradford Dye Reagent (BioRad Laboratories Inc., Hercules, CA, USA). Each protein was detected using an anti-mouse or anti-rabbit IgG horseradish peroxidase-linked whole antibody (GE Healthcare Bio-Science Corp, Piscataway, NJ, USA) and an ECL-PLUS system (GE Healthcare Bio-Science Corp) according to the manufacturer's instructions. Images of bands were acquired by using a digital photo scanner GT-X750 (Seiko Epson Corp, Nagano, Japan). For the cell cycle analysis using flow cytometry, cells were fixed with ice-cold 70%

© 2013 Macmillan Publishers Limited

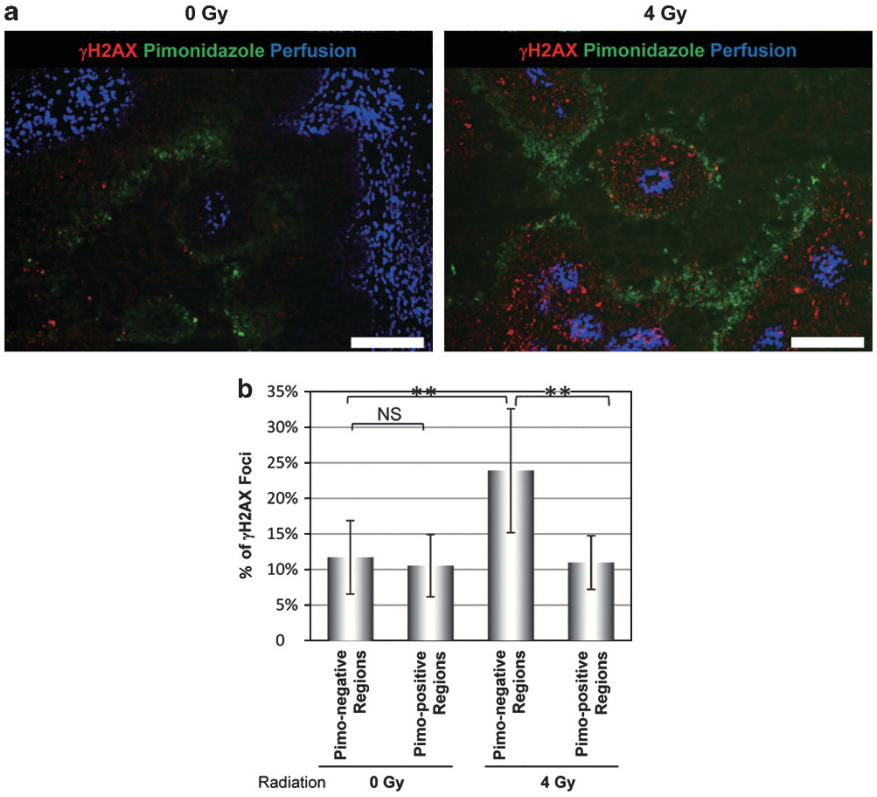

Figure 7. Significant decrease in DNA damage in pimonidazole-positive hypoxic regions. HeLa tumor xenografts were locally treated with ionizing radiation at a dose of 0 or 4 Gy. The xenografts were surgically excised 30 min later, and frozen sections were stained with antibodies against pimonidazole (green) and γH2AX (red). Representative pictures are shown. Blue = perfusion marker, hoechst 33342. Bar = 100 μm. **(b)** Percentages of γ-H2AX-positive cells in pimonidazole-positive regions and pimonidazole-negative regions (excluding necrotic regions) were quantified using the immunohistochemical data in **(a)** after 0 or 4 Gy of radiation. $n = 10$ independent tumor cords. Results are the mean ± s.d. $^{**}P < 0.01$.

ethanol, re-suspended in PBS containing both RNase (1 mg/ml) and propidium iodide (1 mg/ml), incubated at 37 °C for 30 min, and subjected to flow cytometry (BD Bioscience, Franklin Lakes, NJ, USA) as described previously.[50] The results were analyzed with Cell Quest software (BD Bioscience).

Clonogenic survival assay

Cells (2×10^5/35 mm dish) were precultured in medium containing a high (4.5 g/l) or low (0.45 g/l) concentration of glucose under normoxic (20% O_2) or hypoxic (0.02% O_2) conditions for 20 h. The cells were treated with 0, 2, 4 and 8 Gy of X-radiation (Shimadzu, Kyoto, Japan) under the same conditions as for the preculture. The cells were immediately harvested, seeded in 60-mm culture dishes and further cultured for 2 weeks in the CO_2 incubator under normoxic conditions. Surviving colonies were fixed with 70% ethanol and stained with Giemsa solution. Colonies consisting of more than 50 cells were counted as surviving colonies. The plating efficiency and surviving fraction were calculated as described previously.[51]

Tumor-bearing mice, glucagon treatment and radiation treatment *in vivo*

The suspension of HeLa cells (2×10^6 in PBS) was subcutaneously inoculated into the right hind leg of 7-week-old nude mice (BALB/c nu/nu mice; SHIMIZU Laboratory Supplies Co. Ltd, Kyoto, Japan). For the continuous glucagon treatment *in vivo*, an osmotic pump (Alzet Osmotic Pumps: model 1007D, Cupertino, CA, USA) loaded with 2 mg/ml glucagon solution (in 3.44 mM cetrimid solution) was intraperitoneally applied to the tumor-bearing mice. For the radiation treatment *in vivo*, the tumor xenografts were irradiated with the indicated dose of ^{137}Cs γ-rays using a Gammacell 40 Exactor (MDS Nordion International Inc., Ottawa, Ontario, Canada).

Immunohistochemical analyses

HeLa tumor xenografts were surgically excised 90 min after an intraperitoneal injection of pimonidazole hydrochloride (Natural Pharmacia International Inc., Belmont, MA, USA; 60 mg/kg). Then, 30 min before the mice were killed, radiation was given, and 1 min before killing, 100 μl of the perfusion marker Hoechst 33342 trihydrochloride trihydrate solution (10 mg/ml; Invitrogen Corp.) was given. The tumor xenografts were embedded in OCT compound and frozen at − 80 °C. The frozen sections were fixed in acetone and then chloroform for 5 min each, and blocked with blocking solution (serum-free protein block solution (Dako, Glostrup, Denmark) containing 0.1% cold water fish skin gelatin (Sigma-Aldrich Corp.). The sections were treated with the indicated combination of the primary antibodies, such as anti-human HIF-1α rabbit polyclonal antibody (Novus Biologicals, Littleton, CO, USA), anti-pimonidazole mouse monoclonal antibody conjugated with FITC (Natural Pharmacia International Inc.), anti-human γH2AX rabbit antibody (#2577, Cell Signaling Technology Inc.) and anti-human cyclin A rabbit polyclonal antibody (Abcam). HIF-1α was detected with Alexa Fluor 594 goat anti-rabbit IgG (Invitrogen Corp.; in Figure 1a) or with Alexa Fluor 488 goat anti-rabbit IgG (Invitrogen Corp.; in Figure 1b). Cyclin A (in Figure 1b and c) and γH2AX (in Figures 7 and 8) were detected with Alexa Fluor 594 goat anti-rabbit IgG (Invitrogen Corp.). The reproducibility of each staining was confirmed in at least three independent tumors and representative results are shown.

Assay of 53BP1 foci

The 293/EGFP-53BP1-M cells (2×10^5/35 mm collagen-coated dish) were precultured in medium containing a high (4.5 g/l) or low (0.45 g/l) concentration of glucose under normoxic (20% O_2) or hypoxic (0.02% O_2) conditions for 20 h. The cells were treated with 0 or 4 Gy of X-radiation (Shimadzu, Kyoto, Japan) under the same conditions as in the preculture. The EGFP-53BP1-M foci were observed under a fluorescence microscope (IX71, Olympus, Tokyo, Japan) and images were captured using a digital camera (DP72, Olympus) 30 min after the radiation.

© 2013 Macmillan Publishers Limited

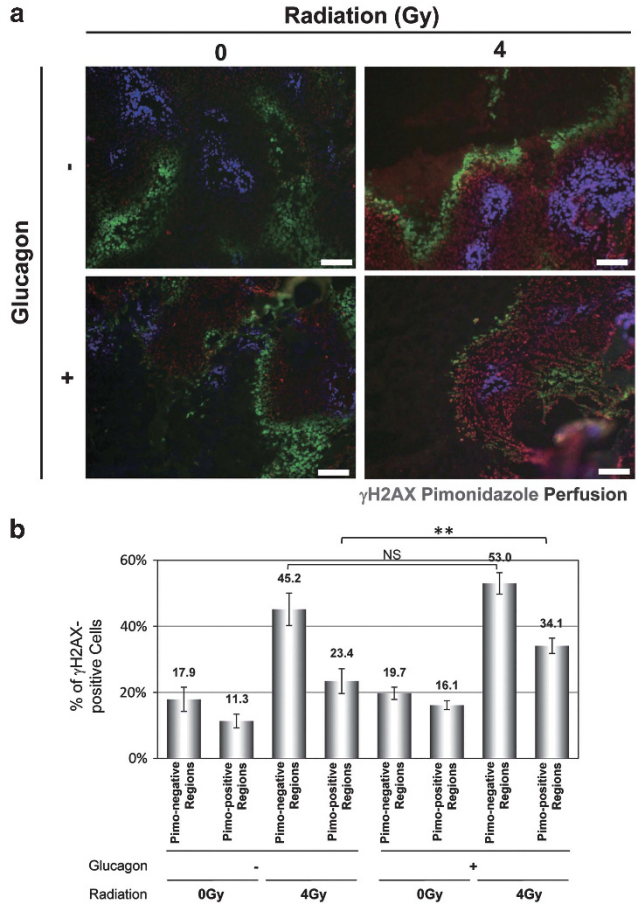

Figure 8. Glucagon-dependent increase of DNA damage in pimonidazole-positive regions. The HeLa tumor-bearing mice were continuously administered with (+) or without (−) glucagon for 5 days via an osmotic pump (see Materials and methods section for details). Then, the xenografts were locally treated with ionizing radiation at a dose of 0 or 4 Gy, and surgically excised 30 min later. The frozen sections were stained with antibodies against pimonidazole (green) and γH2AX (red). The tumor-bearing mice were injected with the hypoxia marker and a perfusion marker, hoechst 33342, at 90 and 1 min before killing, respectively. Representative pictures are shown. Blue = perfusion marker, hoechst 33342. Bar = 100 μm. (**b**). Percentages of γ-H2AX-positive cells in pimonidazole-positive regions and pimonidazole-negative regions (excluding necrotic regions) were quantified using the immunohistochemical data in (**a**) after 0 or 4 Gy of radiation. $n = 10$ independent tumor cords. Results are the mean ± s.d. $^{**}P < 0.01$. NS = not significant.

Statistical Analysis

The statistical significance of differences was determined using Student's *t*-test. A *P* value < 0.05 was considered to be significant.

Ethics of animal experiments

All animal experiments were approved by the Animal Research Committee of Kyoto University.

CONFLICT OF INTEREST

The authors declare no conflict of interest.

ACKNOWLEDGEMENTS

We thank Dr Masahiro Inoue for discussions and Dr GL Semenza for the plasmid pcDNA3-HIF-1α-CA, which expresses the constitutively active mutant form of HIF-1α (HIF-1α-CA). This study was supported by the Funding Program for NEXT Generation World-Leading Researchers (NEXT Program) from the Japan Society for the Promotion of Science (JSPS), Japan to HH (No. LS071), by the Program for Promotion of Fundamental Studies in Health Science from the National Institute of Biomedical Innovation (NIBIO), Japan to HH (No. 09–25), by Grants-in-aid for Young Scientists (B) from the Ministry of Education, Culture, Sports, Science and Technology (MEXT), Japan to HH (No. 21791184). and SI (No. 22791190), by the Sagawa Foundation for the Promotion of Cancer Research to HH, and by the International Science and Technology Cooperation Project of China and Japan to ZL and HH (No. 2010DFA31900).

REFERENCES

1 Deschner EE, Gray LH. Influence of oxygen tension on X-ray-induced chromosomal damage in Ehrlich ascites tumor cells irradiated in vitro and in vivo. *Radiat Res* 1959; **11**: 115–146.
2 Gray LH, Conger AD, Ebert M, Hornsey S, Scott OC. The concentration of oxygen dissolved in tissues at the time of irradiation as a factor in radiotherapy. *Br J Radiol* 1953; **26**: 638–648.
3 Thomlinson RH, Gray LH. The histological structure of some human lung cancers and the possible implications for radiotherapy. *Br J Cancer* 1955; **9**: 539–549.
4 Vaupel P, Kallinowski F, Okunieff P. Blood flow, oxygen and nutrient supply, and metabolic microenvironment of human tumors: a review. *Cancer Res* 1989; **49**: 6449–6465.
5 Brown JM, Wilson WR. Exploiting tumour hypoxia in cancer treatment. *Nat Rev Cancer* 2004; **4**: 437–447.
6 Gorski DH, Beckett MA, Jaskowiak NT, Calvin DP, Mauceri HJ, Salloum RM *et al.* Blockage of the vascular endothelial growth factor stress response increases the antitumor effects of ionizing radiation. *Cancer Res* 1999; **59**: 3374–3378.
7 Moeller BJ, Cao Y, Li CY, Dewhirst MW. Radiation activates HIF-1 to regulate vascular radiosensitivity in tumors: role of reoxygenation, free radicals, and stress granules. *Cancer Cell* 2004; **5**: 429–441.
8 Moeller BJ, Dewhirst MW. Raising the bar: how HIF-1 helps determine tumor radiosensitivity. *Cell Cycle* 2004; **3**: 1107–1110.
9 Aebersold DM, Burri P, Beer KT, Laissue J, Djonov V, Greiner RH *et al.* Expression of hypoxia-inducible factor-1alpha: a novel predictive and prognostic parameter in the radiotherapy of oropharyngeal cancer. *Cancer Res* 2001; **61**: 2911–2916.
10 Irie N, Matsuo T, Nagata I. Protocol of radiotherapy for glioblastoma according to the expression of HIF-1. *Brain Tumor Pathol* 2004; **21**: 1–6.
11 Ishikawa H, Sakurai H, Hasegawa M, Mitsuhashi N, Takahashi M, Masuda N *et al.* Expression of hypoxic-inducible factor 1alpha predicts metastasis-free survival after radiation therapy alone in stage IIIB cervical squamous cell carcinoma. *Int J Radiat Oncol Biol Phys* 2004; **60**: 513–521.
12 Semenza GL. Defining the role of hypoxia-inducible factor 1 in cancer biology and therapeutics. *Oncogene* 2010; **29**: 625–634.
13 Wang GL, Jiang BH, Rue EA, Semenza GL. Hypoxia-inducible factor 1 is a basic-helix-loop-helix-PAS heterodimer regulated by cellular O2 tension. *Proc Natl Acad Sci USA* 1995; **92**: 5510–5514.
14 Berra E, Roux D, Richard DE, Pouyssegur J. Hypoxia-inducible factor-1 alpha (HIF-1 alpha) escapes O(2)-driven proteasomal degradation irrespective of its subcellular localization: nucleus or cytoplasm. *EMBO Rep* 2001; **2**: 615–620.
15 Jaakkola P, Mole DR, Tian YM, Wilson MI, Gielbert J, Gaskell SJ *et al.* Targeting of HIF-alpha to the von Hippel-Lindau ubiquitylation complex by O2-regulated prolyl hydroxylation. *Science* 2001; **292**: 468–472.
16 Semenza GL. Regulation of cancer cell metabolism by hypoxia-inducible factor 1. *Semin Cancer Biol* 2009; **19**: 12–16.
17 Chan DA, Giaccia AJ. Hypoxia, gene expression, and metastasis. *Cancer Metastasis Rev* 2007; **26**: 333–339.
18 Sullivan R, Graham CH. Hypoxia-driven selection of the metastatic phenotype. *Cancer Metastasis Rev* 2007; **26**: 319–331.
19 Forsythe JA, Jiang BH, Iyer NV, Agani F, Leung SW, Koos RD *et al.* Activation of vascular endothelial growth factor gene transcription by hypoxia-inducible factor 1. *Mol Cell Biol* 1996; **16**: 4604–4613.
20 Liao D, Johnson RS. Hypoxia: a key regulator of angiogenesis in cancer. *Cancer Metastasis Rev* 2007; **26**: 281–290.
21 Kizaka-Kondoh S, Inoue M, Harada H, Hiraoka M. Tumor hypoxia: a target for selective cancer therapy. *Cancer Sci* 2003; **94**: 1021–1028.
22 Kizaka-Kondoh S, Konse-Nagasawa H. Significance of nitroimidazole compounds and hypoxia-inducible factor-1 for imaging tumor hypoxia. *Cancer Sci* 2009; **100**: 1366–1373.
23 Kizaka-Kondoh S, Tanaka S, Harada H, Hiraoka M. The HIF-1-active microenvironment: an environmental target for cancer therapy. *Adv Drug Deliv Rev* 2009; **61**: 623–632.

© 2013 Macmillan Publishers Limited

24 Sobhanifar S, Aquino-Parsons C, Stanbridge EJ, Olive P. Reduced expression of hypoxia-inducible factor-1alpha in perinecrotic regions of solid tumors. *Cancer Res* 2005; **65**: 7259–7266.
25 Semenza GL. Hypoxia. Cross talk between oxygen sensing and the cell cycle machinery. *Am J Physiol Cell Physiol* 2011; **301**: C550–C552.
26 Terasima T, Tolmach LJ. Variations in several responses of HeLa cells to x-irradiation during the division cycle. *Biophys J.* 1963; **3**: 11–33.
27 Sinclair WK. Cyclic X-ray responses in mammalian cells in vitro. *Radiat Res* 1968; **33**: 620–643.
28 Palcic B, Skarsgard LD. Reduced oxygen enhancement ratio at low doses of ionizing radiation. *Radiat Res* 1984; **100**: 328–339.
29 Toyoshima H, Hunter T. p27, a novel inhibitor of G1 cyclin-Cdk protein kinase activity, is related to p21. *Cell* 1994; **78**: 67–74.
30 Harada H, Kizaka-Kondoh S, Hiraoka M. Optical imaging of tumor hypoxia and evaluation of efficacy of a hypoxia-targeting drug in living animals. Mol Imaging 2005; **4**: 182–193.
31 Brown JM, Giaccia AJ. The unique physiology of solid tumors: opportunities (and problems) for cancer therapy. *Cancer Res* 1998; **58**: 1408–1416.
32 Tomida A, Tsuruo T. Drug resistance mediated by cellular stress response to the microenvironment of solid tumors. *Anticancer Drug Des* 1999; **14**: 169–177.
33 Li XC, Liao TD, Zhuo JL. Long-term hyperglucagonaemia induces early metabolic and renal phenotypes of Type 2 diabetes in mice. *Clin Sci* 2008; **114**: 591–601.
34 Webb GC, Akbar MS, Zhao C, Swift HH, Steiner DF. Glucagon replacement via micro-osmotic pump corrects hypoglycemia and alpha-cell hyperplasia in pro-hormone convertase 2 knockout mice. *Diabetes* 2002; **51**: 398–405.
35 Anderson L, Henderson C, Adachi Y. Phosphorylation and rapid relocalization of 53BP1 to nuclear foci upon DNA damage. *Mol Cell Biol* 2001; **21**: 1719–1729.
36 Rappold I, Iwabuchi K, Date T, Chen J. Tumor suppressor p53 binding protein 1 (53BP1) is involved in DNA damage-signaling pathways. *J Cell Biol* 2001; **153**: 613–620.
37 Schultz LB, Chehab NH, Malikzay A, Halazonetis TD. p53 binding protein 1 (53BP1) is an early participant in the cellular response to DNA double-strand breaks. *J Cell Biol* 2000; **151**: 1381–1390.
38 Burma S, Chen BP, Murphy M, Kurimasa A, Chen DJ. ATM phosphorylates histone H2AX in response to DNA double-strand breaks. *J Biol Chem* 2001; **276**: 42462–42467.
39 Rogakou EP, Boon C, Redon C, Bonner WM. Megabase chromatin domains involved in DNA double-strand breaks in vivo. *J Cell Biol* 1999; **146**: 905–916.
40 Rogakou EP, Pilch DR, Orr AH, Ivanova VS, Bonner WM. DNA double-stranded breaks induce histone H2AX phosphorylation on serine 139. *J Biol Chem* 1998; **273**: 5858–5868.
41 Pryde F, Khalili S, Robertson K, Selfridge J, Ritchie AM, Melton DW *et al.* 53BP1 exchanges slowly at the sites of DNA damage and appears to require RNA for its association with chromatin. *J Cell Sci* 2005; **118**(Pt 9): 2043–2055.
42 Gardner LB, Li Q, Park MS, Flanagan WM, Semenza GL, Dang CV. Hypoxia inhibits G1/S transition through regulation of p27 expression. *J Biol Chem* 2001; **276**: 7919–7926.
43 Box AH, Demetrick DJ. Cell cycle kinase inhibitor expression and hypoxia-induced cell cycle arrest in human cancer cell lines. *Carcinogenesis* 2004; **25**: 2325–2335.
44 Zeng L, Ou G, Itasaka S, Harada H, Xie X, Shibuya K *et al.* TS-1 enhances the effect of radiotherapy by suppressing radiation-induced hypoxia-inducible factor-1 activation and inducing endothelial cell apoptosis. *Cancer Sci* 2008; **99**: 2327–2335.
45 Harada H, Itasaka S, Zhu Y, Zeng L, Xie X, Morinibu A *et al.* Treatment regimen determines whether an HIF-1 inhibitor enhances or inhibits the effect of radiation therapy. *Br J Cancer* 2009; **100**: 747–757.
46 Brown JMSR. 4233 (tirapazamine): a new anticancer drug exploiting hypoxia in solid tumours. *Br J Cancer* 1993; **67**: 1163–1170.
47 Chen C, Okayama H. High-efficiency transformation of mammalian cells by plasmid DNA. *Mol Cell Biol* 1987; **7**: 2745–2752.
48 Harada H, Itasaka S, Kizaka-Kondoh S, Shibuya K, Morinibu A, Shinomiya K *et al.* The Akt/mTOR pathway assures the synthesis of HIF-1alpha protein in a glucose- and reoxygenation-dependent manner in irradiated tumors. *J Biol Chem* 2009; **284**: 5332–5342.
49 Harada H, Kizaka-Kondoh S, Itasaka S, Shibuya K, Morinibu A, Shinomiya K *et al.* The combination of hypoxia-response enhancers and an oxygen-dependent proteolytic motif enables real-time imaging of absolute HIF-1 activity in tumor xenografts. *Biochem Biophys Res Commun* 2007; **360**: 791–796.
50 Harada H, Kizaka-Kondoh S, Hiraoka M. Mechanism of hypoxia-specific cytotoxicity of procaspase-3 fused with a VHL-mediated protein destruction motif of HIF-1alpha containing Pro564. *FEBS Lett* 2006; **580**: 5718–5722.
51 Franken NA, Rodermond HM, Stap J, Haveman J, van Bree C. Clonogenic assay of cells in vitro. *Nat Protoc* 2006; **1**: 2315–2319.

This work is licensed under the Creative Commons Attribution-NonCommercial-No Derivative Works 3.0 Unported License. To view a copy of this license, visit http://creativecommons.org/licenses/by-nc-nd/3.0/

Supplementary Information accompanies the paper on the Oncogene website (http://www.nature.com/onc)

© 2013 Macmillan Publishers Limited